Androgen receptor drives lenvatinib resistance in hepatocellular carcinoma through transcriptional activation of EIF3I and a downstream ceRNA axis

CHANGFENG LIU, BING ZHANG, YE JIN, ZHI CHEN, MIAOMIAO WANG and ZUJIAN WU

General Surgery Research Laboratory, Department of Hepatobiliary and Pancreatic Surgery, Tongde Hospital of Zhejiang Province, Hangzhou, Zhejiang 310012, P.R. China

Received December 10, 2025; Accepted May 22, 2026

DOI: 10.3892/ol.2026.15725

Abstract. Lenvatinib resistance is a notable clinical challenge in advanced hepatocellular carcinoma (HCC). Androgen receptor (AR) upregulation has been associated with poor prognosis and high invasiveness, particularly in AR-high HCC, yet its specific role in lenvatinib resistance remains unclear. The present study investigated whether AR confers resistance through regulating the circular RNA hsa_circ_0011385. Bioinformatic screening and experimental validation identified hsa_circ_0011385 as significantly upregulated in HCC tissues and AR-high cell lines. In established lenvatinib-resistant cells (MHCC97H-LR), AR, hsa_circ_0011385 and Akt3 were upregulated, while miR-212-5p was downregulated. Mechanistically, AR directly bound to the promoter of eukaryotic translation initiation factor 3 subunit I (EIF3I), the host gene of hsa_circ_0011385 and promoted its transcription. The upregulated hsa_circ_0011385 acted as a molecular sponge for miR-212-5p, thereby relieving its inhibition of the downstream oncogene Akt3. Functional assays showed that AR knockdown sensitized resistant cells to lenvatinib, inhibiting proliferation and migration while promoting apoptosis, whereas overexpressing hsa_circ_0011385 reversed these effects. To the best of our knowledge, the present study revealed for the first time that in AR-high HCC, AR drives lenvatinib resistance by activating the EIF3I/hsa_circ_0011385/miR-212-5p/Akt3 axis. This finding provides a new theoretical basis and potential therapeutic targets for overcoming lenvatinib resistance in this patient subset.

Correspondence to: Dr Changfeng Liu or Dr Zujian Wu, General Surgery Research Laboratory, Department of Hepatobiliary and Pancreatic Surgery, Tongde Hospital of Zhejiang Province, 234 Gucui Road, Hangzhou, Zhejiang 310012, P.R. China
E-mail: laochunteng@163.com
E-mail: wuzujian1996@126.com

Key words: hepatocellular carcinoma, lenvatinib resistance, androgen receptor, hsa_circ_0011385, transcriptional activation, competing endogenous RNA

Introduction

Globally, cancer-associated mortality is dominated by liver cancer, the burden of which is continually rising. For instance, liver cancer accounted for ~758,000 deaths (7.8% of all cancer deaths) in 2022, ranking as the third leading cause of cancer death worldwide (1). Moreover, between 2020 and 2040, new liver cancer cases and deaths are projected to increase by >55% (2). The majority of patients with hepatocellular carcinoma (HCC) are diagnosed at an advanced stage, thereby may not get the opportunity to undergo curative treatments (3). Molecular targeted drugs, including lenvatinib, may bring hope to patients with advanced HCC. However, lenvatinib resistance has been widely reported, representing a new challenge in HCC clinical management (4,5).

As a broad-spectrum tyrosine kinase inhibitor, lenvatinib antagonizes VEGFR, fibroblast growth factor receptor (FGFR) and platelet-derived growth factor receptor families and associated kinases (rearranged during transfection and c-Kit, among others), which curtails neovascularization and cancer cell expansion (6). Its resistance mechanisms involve the synergistic action of numerous pathways, including c-Myc, Wnt/β-catenin and PI3K/AKT signaling (7-9).

Novel observations have revealed the pivotal role of circular RNAs (circRNAs) in mediating lenvatinib refractoriness as they can indirectly regulate gene expression as 'micro (mi)-RNA sponges' or directly bind to and modify key signaling proteins (such as GSK3β and PSIP1) as 'protein function modulators', enhancing cancer stem cell stemness and driving resistance by activating core pathways such as c-Myc or Wnt/β-catenin (7-9).

Androgen receptor (AR) expression has shown marked heterogeneity in HCC. High-metastasis cell lines such as MHCC97L and HCCLM3 exhibit high AR expression, whereas epithelial cell lines including HepG2 and Huh7 show nearly undetectable AR protein levels. This expression pattern implies a potential association between elevated AR levels and HCC invasion and metastasis (10-12). A recent study further indicated that high AR expression is also associated with lenvatinib resistance, whereby in AR-high, α-fetoprotein (AFP)-negative HCC models, AR can promote angiogenesis, leading to the failure of lenvatinib monotherapy, while

combination therapy with the AR antagonist bicalutamide has been shown to notably restore its antitumor and anti-angiogenic effects (11). However, this mechanism primarily focuses on vascular microenvironment remodeling. Whether AR drives lenvatinib resistance through other pathways remains to be elucidated. Therefore, the present study investigated, from the perspective of circRNA, the transcriptional regulatory role of AR on circRNAs, with the aim of revealing a novel molecular mechanism underlying AR-high-mediated lenvatinib resistance.

Bioinformatic analysis has suggested that AR may be a potential transcriptional regulator of host genes for a number of differentially expressed circRNAs in HCC. Among them, hsa_circ_0011385 and hsa_circ_0001955 have been demonstrated to be highly expressed in HCC, promoting HCC cell proliferation and metastasis (13-16). miRNA-212-5p (miR-212-5p), a potential target of hsa_circ_0011385 downregulated in hepatitis B virus-associated HCC, is considered an effective biomarker for early HCC diagnosis and has also been shown to inhibit HCC progression. Akt is at the hub of the PI3K/Akt/mTOR network and is hyperactivated by receptor tyrosine kinases, including EGFR, MET and FGFR, thereby accelerating hepatocellular carcinoma progression. Furthermore, sustained Akt activation is a key driver of acquired lenvatinib resistance and Akt inhibitors can reverse this resistance (17-19). Akt3, a key Akt isoform potentially controlled by miR-212-5p, has been repeatedly implicated in HCC progression (20,21).

Based on these findings, the present study hypothesized that AR, through its transcription factor function, may regulate the transcription of EIF3I, which generates hsa_circ_0011385 and thus alter the level of this circRNA. Hsa_circ_0011385 sequesters miR-212-5p, thereby easing the repression of the downstream oncogene Akt3 and ultimately promoting lenvatinib resistance in HCC. The present study aimed to validate this molecular mechanism using the AR-high cell line MHCC97H as the research model.

Materials and methods

Bioinformatic analysis. Raw circRNA expression matrices for HCC were downloaded from the Gene Expression Omnibus (GEO) database (https://www.ncbi.nlm.nih.gov/geo) by using 'circRNA' and 'hepatocellular carcinoma' as search terms. Two GEO datasets, GSE97332 (circRNA expression in HCC and matched non-tumor tissues) (22) and GSE242797 (construct a ceRNA regulatory network to explore potential pathogenesis and therapy options of human hepatocellular carcinoma) (23), were used for differential expression analysis. The names of the circRNAs were standardized according to the circBase database (http://www.circbase.org/). The differential expression of circRNAs was analysed by the R package 'limma' (version 4.2.2; Posit Software, PBC) with log2 (fold-change) >1.5 and P<0.05 (24). Host gene promoter sequences were obtained from the University of California, Santa Cruz database (https://genome.ucsc.edu/) and subsequently submitted to the JASPAR database (https://jaspar.elixir.no/) to predict potential AR binding sites. The Cancer Genome Atlas (TCGA) database (https://www.cancer.gov/tcga) data were analyzed using the University of Alabama at Birmingham Cancer data analysis portal online tool (http://ualcan.path.uab.edu) to assess differential gene expression. The median expression value was used as the cutoff to define high- and low-expression groups.

Cell culture and transfection. THLE-2 normal hepatocytes and liver cancer cell lines MHCC97H, HCCLM3 and HepG2 were obtained from iCell Bioscience Inc. Short tandem repeat profiling was performed externally by the cell supplier to confirm the identity of each line, and all tested negative for *Mycoplasma*. Using DMEM (Gibco; Thermo Fisher Scientific, Inc.) supplemented with 10% FBS (Gibco; Thermo Fisher Scientific, Inc.), cells were kept at 37˚C with 5% CO_2 in a humidified incubator. For overexpression, the hsa_circ_0011385 sequence was cloned into the pCD2.1-ciR circRNA expression vector (Guangzhou Geneseed Biotech. Co., Ltd.) using 50 ng of vector per ligation reaction and a 3:1 molar ratio of insert to vector, as recommended by standard protocols. Cells transfected with the corresponding empty vector were used as the negative control in these experiments. Small interfering RNA (siRNA), overexpression plasmids and corresponding control vectors were manufactured by Wuhan GeneCreate Biological Engineering Co., Ltd. Lipofectamine™ 2000 (Invitrogen; Thermo Fisher Scientific, Inc.) was used for cell transfection in complete compliance with the manufacturer's instructions. The sequences used were as follows: AR-si1 sense: 5'-GGUUCAACAGUCCACAATT-3', antisense: 5'-UUGGUGAGUGGUAGAAGCTT-3'; AR-si2 sense: 5'-CUGAUCUGUGGAGAUGAATT-3', antisense: 5'-UCAUCUCACAGAUCAGTT-3'; AR-si3 sense: 5'-GCAAGGUUGUGCUAGUATT-3', antisense: 5'-UACUAGCACAAGCUUGCTT-3'; si-negative control sense: 5'-UUCUCCGAACGUGUCACGUTT-3'. Among these, si-AR-3 exhibited the most potent AR knock-down and was therefore selected for all subsequent functional experiments, which were performed at 48 h post-transfection.

Establishment of lenvatinib-resistant cell line. Lenvatinib was purchased from Beyotime Biotechnology. A lenvatinib-resistant cell line was generated using a stepwise concentration-increasing method. MHCC97H cells at logarithmic growth phase were treated with a starting concentration of ~10 μM (half of the 72-h IC_{50} value). The concentration was doubled every 2-3 weeks until reaching 80 μM and cells were then stably passaged at this concentration for 4 weeks. Throughout the procedure, cells were maintained in a 5% CO_2 humidified incubator at 37˚C, with drug-containing medium refreshed every 48 h. Cells were passaged upon reaching ~90% confluence. The entire induction process lasted ~4 months. The final resistant cell line obtained was named MHCC97H-LR (lenvatinib-resistant).

Enzalutamide treatment. MHCC97H cells were seeded in 6-well plates at a density of $3x10^5$ cells per well and cultured overnight. Cells were then treated with 10 μM enzalutamide (SC0074-10 mM; Beyotime Biotechnology) at 37˚C for 48 h. Control cells were treated with DMSO (cat. no. ST038; Beyotime Biotechnology) at a final concentration of 0.1% at 37˚C. After 48 h, cells were harvested for RNA extraction.

Table I. Primer sequences.

Primer	Sequence (5'-3')
GAPDH-F	GGAGCGAGATCCCTCCAAAAT
GAPDH-R	GGCTGTTGTCATACTTCTCATGG
AR-F	CCAGGGACCATGTTTTGCC
AR-R	CGAAGACGACAAGATGGACAA
hsa_circ_0011385-F	ATAGTGCCAAGGAAAGC
hsa_circ_0011385-R	TGTCCGTGGAGAACAT
hsa_circ_0001955-F	AAATCAGGTGAAGGTC
hsa_circ_0001955-R	CACATGGTCCAAAGTA
hsa-miR-212-5p-F	CGCGACCTTGGCTCTAGACTG
hsa-miR-212-5p-R	AGTGCAGGGTCCGAGGTATT
hsa-miR-212-5p RT	GTCGTATCCAGTGCAGGGTCCGAGGTATTCGCACTGGATACGACAGTAAG
U6-F	CTCGCTTCGGCAGCACA
U6-R	AACGCTTCACGAATTTGCGT
Akt3-F	AATGGACAGAAGCTATCCAGGC
Akt3-R	TGATGGGTTGTAGAGGCATCC
EIF3I-F	CTCAAGACCAATTCGGCTGTC
EIF3I-R	CTGGTAGCCCATCTGCTTGTC
CSNK1G1-F	CCATCACAACAGCAGCCTCTTC
CSNK1G1-R	CTTCCTCCACTACCTCCACCTC

CSNK1G1, casein kinase 1 γ-1; F, forward; R, reverse; AR, androgen receptor; circ, circular RNA; miR, microRNA; EIF3I, eukaryotic translation initiation factor 3 subunit I; RT, reverse transcription.

RNA extraction and reverse transcription-quantitative PCR (RT-qPCR). Cells from all experimental groups (including normal hepatocytes, HCC cell lines, lenvatinib-resistant cells and transfected cells) were lysed for total RNA or miRNA isolation with the Animal Total RNA Isolation Kit (cat. no. RE-03011; Chengdu Fuji Biotechnology Co., Ltd.) according to the manufacturer's instructions and the yield stored at -80˚C. miRNA was reverse-transcribed with the SeqHunt® First Strand cDNA Synthesis Kit (cat. no. CA01; Seq-Hunt Biotechnology Co., Ltd.). mRNA and microRNA levels were then quantified by RT-qPCR using 2x Blue Universal SYBR qPCR Master Mix (cat. no. AF07; Seq-Hunt Biotechnology Co., Ltd.) with GAPDH and U6 as the respective internal controls. The thermocycling conditions were as follows: 95˚C for 5 min, followed by 40 cycles of 95˚C for 15 sec and 60˚C for 40 sec. Expression ratios were calculated using the $2^{-\Delta\Delta Cq}$ method (25) and primer sequences are provided in Table I.

Cell Counting Kit-8 (CCK-8) proliferation assay. To perform this assay, an optimal density of cells was seeded into 96-well plates and incubated overnight at 37˚C under 5% CO_2 to ensure adherence. Following a 24-h exposure to 100 μl serially diluted drug (under identical culture conditions), cell viability was assessed. Specifically, 10 μl CCK-8 reagent (cat. no. CK04; Dojindo Laboratories, Inc.) was introduced per well and the plates were returned to the 37˚C incubator for a 1 to 2-h development period. The reaction was then stopped by immediate mixing after adding 10 μl stop solution to each well. Finally, absorbance at 450 nm was recorded using a microplate reader (TMR-100; Tuoh Electromechanical Technology Co., Ltd.).

Transwell migration assay. Following digestion and harvesting, cells were resuspended in serum-free DMEM (Gibco; Thermo Fisher Scientific, Inc.) for subsequent counting. A cellular suspension containing $1x10^4$ cells in 100 μl was applied to the upper chamber of a Transwell insert. Meanwhile, the lower compartment received 600 μl of complete medium supplemented with 10% FBS. After a 24-h incubation at 37˚C and 5% CO_2, the insert was carefully withdrawn. Stationary cells remaining on the upper membrane surface were then cleared away. Subsequent steps for the migrated cells on the lower membrane involved sequential processing: First, fixation in 4% paraformaldehyde (15 min), followed by staining with crystal violet (20 min), both at room temperature, followed by two washes with PBS (cat. no. BL302; Biosharp Life Sciences). Finally, the membranes were examined and photographed using an inverted MI40 microscope (Guangzhou Micro-Shot Technology Co., Ltd).

Flow cytometric analysis of apoptosis. Apoptosis was detected by flow cytometry using the Annexin V-FITC/PI double-staining method, with experimental procedures strictly following the kit instructions (cat. no. KTA0004; Abbkine, Inc.). Briefly, after discarding the cell culture medium and collecting the supernatant, cells were gently washed twice with pre-chilled PBS. Digestion was performed using 0.25% EDTA-free trypsin, which was then terminated by adding complete medium containing 10% FBS, followed by gentle pipetting to obtain a single-cell suspension. The suspension was centrifuged at 120 x g for 5 min at room temperature. After discarding the supernatant, the cell pellet was resuspended in

Table II. Antibodies used for western blotting analysis.

Target/purpose	Cat. no.	Supplier	Dilution
AR	22089-1-AP	Proteintech Group, Inc.	1:5,000
Akt3	21641-1-AP	Proteintech Group, Inc.	1:1,000
EIF3I	11287-1-AP	Proteintech Group, Inc.	1:1,000
GAPDH (loading control)	60004-1-Ig	Proteintech Group, Inc.	1:50,000
HRP-conjugated Goat Anti-Rabbit IgG	A21020	Abbkine, Inc.	1:10,000
HRP-conjugated Goat Anti-Mouse IgG	A21010	Abbkine, Inc.	1:10,000

AR, androgen receptor; EIF3I, eukaryotic translation initiation factor 3 subunit I.

pre-chilled 1x PBS and washed twice again. Subsequently, cells were resuspended in pre-chilled 1x Annexin V binding buffer and adjusted to a density of $1x10^6$ cells/ml. A 100 μl aliquot of the cell suspension was taken and 5 μl Annexin V-FITC and 10 μl PI staining solution were added sequentially, followed by incubation at room temperature in the dark for 15 min. Finally, 400 μl binding buffer was added to each tube and samples were immediately analyzed using a flow cytometer (CytoFLEX; Beckman Coulter, Inc.). Data analysis was performed using CytExpert software (version 2.5; Beckman Coulter, Inc.).

Dual-luciferase reporter assay. For hsa_circ_0011385 and the Akt3 3'-untranslated region (UTR), luciferase reporters carrying either wild-type (WT) or mutant (MT) fragments were generated and named circ_0011385-WT, circ_0011385-MT, Akt3-WT and Akt3-MT, respectively. All constructs were sequence-verified prior to use. Subsequently, 293T cells were co-transfected with these reporters together with hsa-miR-212-5p mimics using the same transfection protocol as aforementioned (Lipofectamine 2000; Invitrogen; Thermo Fisher Scientific, Inc.); 48 h later, firefly and *Renilla* activities were quantified with the Dual-Luciferase Reporter Assay Kit (cat. no. JKR23008; Wuhan GeneCreate Biological Engineering Co., Ltd.). The miR-212-5p mimics (sense: 5'-ACC UUGGCUCUAGACUGCUUACU-3', antisense: 5'-AGUAAG CAGUCUAGAGCCAAGGU-3') and NC mimics (sense: 5 -UCACAACCUCCUAGAAAGAGUAGA-3', antisense: 5'-UCUACUCUUUCUAGGAGGUUGUGA-3') were utilized in the present study.

Chromatin immunoprecipitation-qPCR (ChIP-qPCR). Chromatin immunoprecipitation was carried out using the ChIP Kit (cat. no. JKR23002A; Wuhan GeneCreate Biological Engineering Co., Ltd.). After 10 min cross-linking with 1% formaldehyde, the cross-linking reaction was quenched through a 5-min incubation with 0.125 M glycine at room temperature. Subsequent to two washes with PBS, cells were pelleted by centrifugation at 1,000 x g for 5 min at 4˚C and rapidly frozen at -80˚C. For chromatin lysis, cells were resuspended in Lysis Buffer provided in the ChIP Kit (cat. no. JKR23002A; Wuhan GeneCreate Biological Engineering Co., Ltd.), supplemented with 1X Protease Inhibitor and 5 μl DTT according to the manufacturer's protocol. A 10-min lysis step was performed on ice. After centrifugation at 12,000 x g for 10 min at 4˚C to pellet debris and remove the supernatant, the pellet was subjected to a second lysis and sonication. Chromatin fragments were then incubated with either AR antibody (cat. no. 22089-1-AP; Proteintech Group, Inc.) or control immunoglobulin G (normal rabbit IgG; cat. no. F040301; Beyotime Biotechnology), both used at a final concentration of 1 μg/ml, overnight at 4˚C. After elution and reversal of cross-links (65˚C, overnight), DNA was purified according to the kit protocol and analysed by RT-qPCR with primers specific for the EIF3I promoter region. The primer sequences used were as follows: Primer 1: forward 5'-TGCCAGGCACTCTCCTAGAT-3' and reverse 5'-GTT GGTTTGAAGCCTGGCAG-3'; primer 2: forward 5'-CTG CCAGGCTTCAAACCAAC-3' and reverse 5'-GTTTGAGGC CACCTGGAAGA-3'; and primer 3: forward 5'-CACAGA GACGCACCTCAGTAT-3' and reverse 5'-TGACTCACTCGT CTGCATTC-3'.

Western blotting. Western blotting was performed as follows: Proteins were extracted from cells using RIPA buffer (cat. no. BL504A; Biosharp Life Sciences), quantified by BCA (BL521A; Biosharp Life Sciences) and 20 μg was denatured and separated by 10% SDS-PAGE (80/120 V). Proteins were wet-transferred (200 mA; 90 min; ice bath) to PVDF membranes (0.22 μm). After blocking (5% skimmed milk in TBST with 0.1% Tween-20; 1 h; room temperature), membranes were probed with primary antibodies (1:1,000-1:50,000 in 1% BSA-PBST; 4˚C; overnight) and HRP-secondary antibodies (1:10,000 in 5% skim milk-PBST; 1 h; room temperature), with PBST washes between steps. Detection was conducted with the SuperKine™ West Pico PLUS Chemiluminescent Substrate (cat. no. BMU101-CN; Abbkine, Inc.; 1.5 min) and a ChemiScope 6100T imager (Clinx Science Instruments Co., Ltd.). Detailed information on the antibodies used is provided in Table II.

Statistical analysis. After determining parametric assumptions (normality by Shapiro-Wilk test and homogeneity of variances by Levene's test), pairwise comparisons were analyzed using unpaired Student's t tests. Multi-factor datasets were analyzed using one-way ANOVAs followed by Tukey's multiple-comparison tests, except for CCK-8 data which were analyzed by two-way ANOVA followed by Tukey's test. Data are presented as the mean ± SD from at least three independent experiments. $P<0.05$ was considered to indicate a statistically significant difference. All statistical analyses were performed

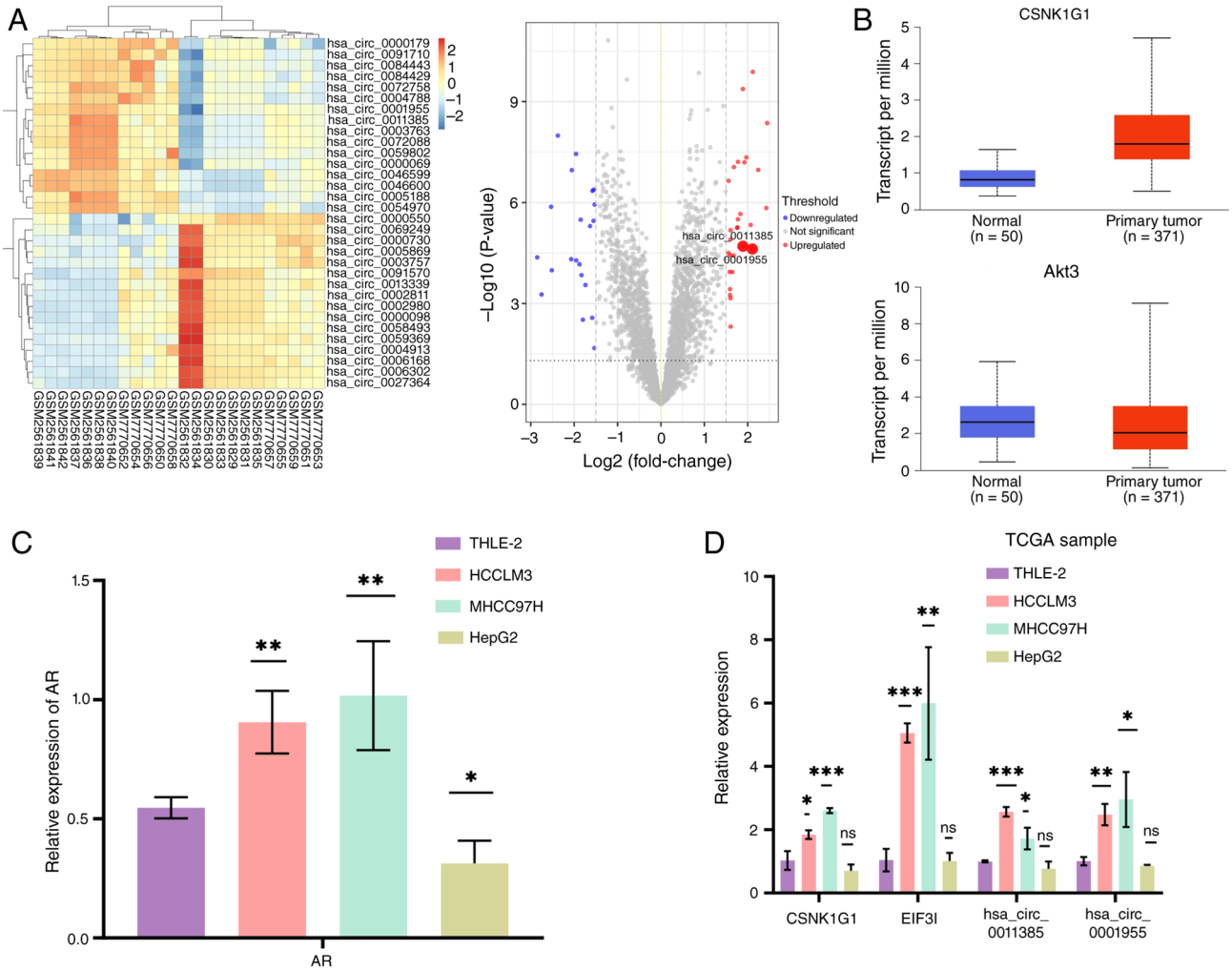

Figure 1. Identification of AR-regulated candidate circRNAs in HCC. (A) Heatmap and volcano plot illustrating circRNA expression changes in HCC relative to matched non-tumour specimens deposited under Gene Expression Omnibus: GSE242797 and GSE97332. The volcano plot highlights key circRNAs (hsa_circ_0011385 and hsa_circ_0001955) with larger circles. Thresholds for significance were set at log2 (fold-change) >1.5 and adjusted P<0.05. Red, green and gray dots represent significantly upregulated, downregulated and non-significant circRNAs, respectively. (B) Analysis of TCGA data shows high expression of circRNAs hsa_circ_0001955 (host gene: CSNK1G1) and hsa_circ_0011385 (host gene: EIF3I) in HCC. (C) RT-qPCR analysis of AR mRNA expression in THLE-2 normal hepatocytes and HCC cell lines (HepG2, MHCC97H and HCCLM3). (D) RT-qPCR determined the abundance of hsa_circ_0001955 and hsa_circ_0011385 in THLE-2 normal hepatocytes compared with the HCC models MHCC97H, HCCLM3 and HepG2. Data are presented as the mean ± SD from three independent experiments. *P<0.05, **P<0.01 and ***P<0.001 vs. THLE-2. AR, androgen receptor; circRNA, circular RNA; HCC, hepatocellular carcinoma; TCGA, The Cancer Genome Atlas; RT-qPCR, reverse transcription-quantitative PCR; CSNK1G1, casein kinase 1 γ-1; ns, not significant; LIHC, liver hepatocellular carcinoma; EIF3I, eukaryotic translation initiation factor 3 subunit I.

using GraphPad Prism (version 7.0; Dotmatics), R software (version 4.2.2; Posit Software, PBC) or SPSS Statistics (version 24; IBM, Corp.).

Results

Bioinformatic screening identifies AR-regulated candidate circRNAs. Preliminary bioinformatic analysis of GEO microarray datasets (GSE97332 and GSE242797) identified 16 significantly upregulated and 16 significantly downregulated circRNAs in HCC tissues compared with paired normal tissues (log_2 FC >1.5; P<0.05), visualized as a heatmap and volcano plot (Fig. 1A). Analysis of TCGA data revealed high expression of two circRNAs previously implicated in HCC (13-16) along with their corresponding host genes: hsa_circ_0001955 [casein kinase 1 γ-1 (CSNK1G1)] and hsa_circ_0011385 (EIF3I; Fig. 1B). RT-qPCR analysis of AR expression in the same cell lines showed that, compared with THLE-2 normal hepatocytes, MHCC97H and HCCLM3 cell lines expressed significantly higher AR mRNA levels, whereas HepG2 cells exhibited the lowest AR expression (Fig. 1C). RT-qPCR determined that, relative to normal THLE-2 hepatocytes, hsa_circ_0001955 (CSNK1G1) and hsa_circ_0011385 (EIF3I) exhibited markedly elevated levels in MHCC97H and HCCLM3 cells, whereas HepG2 cells exhibited only faint expression (Fig. 1D).

Establishment of lenvatinib-resistant cells and expression changes in the AR/hsa_circ_0011385/miR-212-5p/Akt3 axis. MHCC97H-LR, a lenvatinib-resistant HCC derivative, was obtained by stepwise escalation of drug concentration. Relative to the parental population, the selected line exhibited markedly reduced lenvatinib sensitivity: IC_{50} increased from 19.7-25.7 to 63.0-79.6 μM, giving a 3.1-fold resistance index (Fig. 2A). In

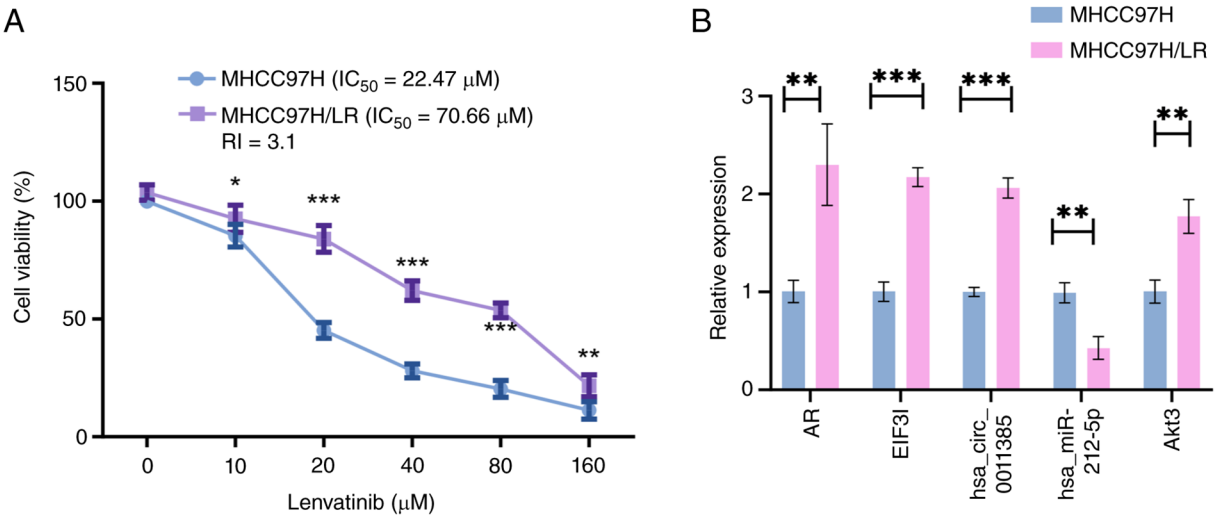

Figure 2. Establishment of lenvatinib-resistant hepatocellular carcinoma cells and expression profiling of the AR axis. (A) Dose-response curves of parental MHCC97H and lenvatinib-resistant MHCC97H-LR cells treated with lenvatinib for 72 h (Cell Counting Kit-8 assay). The IC_{50} values and RI are indicated. (B) Reverse transcription-quantitative PCR analysis of AR, hsa_circ_0011385 (EIF3I), miR-212-5p and Akt3 mRNA expression levels in MHCC97H and MHCC97H-LR cells. Data are presented as the mean ± SD from three independent experiments. *P<0.05, **P<0.01 and ***P<0.001. LR, lenvatinib-resistant; RI, resistance index; miR, microRNA; AR, androgen receptor; EIF3I, eukaryotic translation initiation factor 3 subunit I.

these resistant cells, AR, Akt3 and hsa_circ_0011385 (EIF3I) were upregulated, while hsa-miR-212-5p expression was downregulated (Fig. 2B).

Expression changes in the hsa_circ_0011385/miR-212-5p/Akt3 axis following AR inhibition. RT-qPCR showed that compared with the THLE-2 cell line, MHCC97H cells exhibited significantly higher expression of AR, hsa_circ_0011385, its host gene EIF3I and the downstream target gene Akt3, while hsa-miR-212-5p expression was significantly lower (Fig. 3A). RT-qPCR demonstrated an inhibitory effect after AR siRNA silencing (Fig. 3B) and showed that AR knockdown in MHCC97H cells led to significant downregulation of Akt3 and hsa_circ_0011385 (EIF3I) expression and significant upregulation of hsa-miR-212-5p expression (Fig. 3C). Western blotting analysis determined significantly higher protein expression of AR, EIF3I and Akt3 in MHCC97H cells compared with THLE-2 cells and demonstrated that AR knockdown relatively reduced EIF3I and Akt3 protein levels (Fig. 3D).

Validation of the targeting regulatory association within the AR/hsa_circ_0011385/miR-212-5p/Akt3 axis. To define how AR regulates hsa_circ_0011385, the EIF3I promoter (source of circ_0011385) was scanned in JASPAR for AR motifs (Fig. 4A). ChIP-qPCR with three primer pairs verified strong AR enrichment at the predicted sites (Fig. 4B). Dual-luciferase assays showed that miR-212-5p directly bound circ_0011385-WT and Akt3-WT, reducing their reporter signals (Fig. 4C). To validate AR transcriptional regulation, MHCC97H cells were treated with the AR antagonist enzalutamide. Enzalutamide significantly reduced EIF3I mRNA and hsa_circ_0011385 levels compared with DMSO control (Fig. 4D), consistent with the ChIP-qPCR results. These findings determined a targeted regulatory cascade within the AR/hsa_circ_0011385/miR-212-5p/Akt3 axis.

Low AR expression attenuates the biological activity of lenvatinib-resistant MHCC97H cells and hsa_circ_0011385 overexpression reverses the effects of AR knockdown on lenvatinib resistance. RT-qPCR validated the overexpression effect of hsa_circ_0011385 (Fig. 5A). CCK-8 assay results showed that compared with parental MHCC97H cells, lenvatinib-resistant cells exhibited significantly enhanced proliferation capacity, which was significantly weakened upon AR interference (Fig. 5B). Transwell assays exhibited a similar trend with lenvatinib-resistant cells displaying strong migration capacity, which was reduced after AR interference (Fig. 5C). Flow cytometric apoptosis assays indicated that compared with MHCC97H, resistant cells exhibited a decreased apoptosis rate, which significantly increased after AR interference (Fig. 5D). Overexpression of hsa_circ_0011385 significantly reversed the inhibitory effects caused by AR knockdown.

MiR-212-5p directly modulates Akt3 expression and lenvatinib sensitivity in resistant cells. To provide direct functional evidence for the role of miR-212-5p in lenvatinib resistance, MHCC97H-LR cells were transfected with miR-212-5p mimic or inhibitor. RT-qPCR and western blotting analyses showed that miR-212-5p mimic significantly downregulated Akt3 expression at both mRNA and protein levels, whereas miR-212-5p inhibitor upregulated Akt3 expression (Fig. 6A and B). The CCK-8 assay demonstrated that the miR-212-5p mimic suppressed the proliferation of lenvatinib-resistant MHCC97H-LR cells, while miR-212-5p inhibitor further enhanced proliferation (Fig. 6C). Flow cytometric apoptosis analysis revealed that miR-212-5p mimic increased the apoptosis rate, whereas miR-212-5p inhibitor decreased apoptosis in resistant cells (Fig. 6D). These results determined that miR-212-5p directly regulated Akt3 expression and lenvatinib sensitivity, supporting the proposed competing endogenous RNA (ceRNA) mechanism.

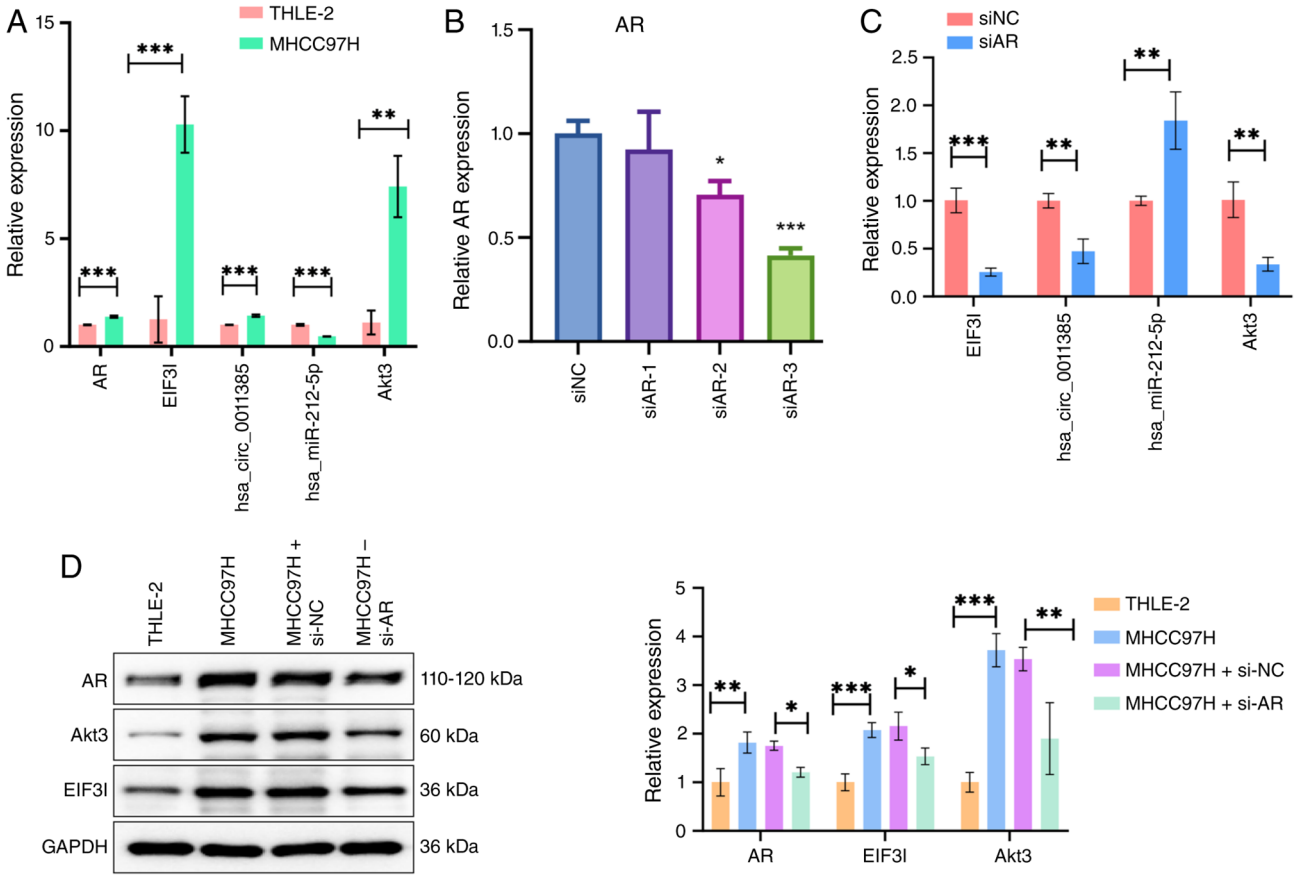

Figure 3. AR modulates the expression of the hsa_circ_0011385/miR-212-5p/Akt3 axis. (A) RT-qPCR analysis of AR, EIF3I, hsa_circ_0011385, miR-212-5p and Akt3 expression in THLE-2 and MHCC97H cells. (B) RT-qPCR determining efficient knockdown of AR by siRNA in MHCC97H cells. (C) RT-qPCR demonstrating the effects of AR knockdown on the expression of hsa_circ_0011385 (EIF3I), miR-212-5p and Akt3. (D) Western blotting analysis of AR, EIF3I and Akt3 protein levels in THLE-2, MHCC97H and AR-knockdown MHCC97H cells. GAPDH served as the loading control. Data are presented as the mean ± SD from three independent experiments. *P<0.05, **P<0.01 and ***P<0.001. AR, androgen receptor; EIF3I, eukaryotic translation initiation factor 3 subunit I; RT-qPCR, reverse transcription-quantitative PCR; miR, microRNA; si/siRNA, small interfering RNA; NC, negative control.

Discussion

Acquired resistance to lenvatinib is a marked clinical challenge in the treatment of advanced HCC. Recent studies have identified AR as a pro-oncogenic factor in HCC, whose activation contributes to cell proliferation and angiogenesis and may be associated with lenvatinib resistance (11,26,27). The present study revealed that in the AR-high HCC subset, AR drives lenvatinib resistance by directly transcriptionally upregulating the circRNA hsa_circ_0011385, which then acts as a 'molecular sponge' for miR-212-5p, relieving its inhibition of the downstream oncogene Akt3. This finding provides a new molecular perspective for understanding the poor prognosis of patients with high AR expression.

In recent years, the role of circRNAs in HCC drug resistance has been increasingly uncovered. A number of studies have determined that circRNAs confer acquired lenvatinib resistance in HCC by sponging tumor-suppressive miRNAs or acting as scaffolds to activate pathways such as c-Myc/β-catenin/EGFR, rapidly rebuilding VEGF-independent angiogenesis and tumor stemness (7-9,28,29). These key discoveries collectively established the research foundation for circRNAs in the field of drug resistance. The importance of the present study lies not only in identifying another functionally unknown resistance-associated circRNA, but in associating the transcriptional regulatory function of AR with circRNA dysregulation in a specific cellular context, thereby revealing a previously unclear molecular pathway through which high AR expression leads to lenvatinib resistance.

In the successfully established lenvatinib-resistant cell model, the present study demonstrated coordinated dysregulation of the AR/hsa_circ_0011385/miR-212-5p/Akt3 axis in resistant cells. At the mechanistic level, the present study clarified the causal associations within this axis. Upstream, ChIP-qPCR experiments provided key evidence for the direct binding of AR to the EIF3I promoter. To the best of our knowledge, the present study is the first to propose an explanation of the upregulation mechanism of hsa_circ_0011385 at the transcriptional initiation level: AR promotes the transcription of its host gene EIF3I, providing a richer pool of precursor mRNA templates for the back-splicing of hsa_circ_0011385, which is the primary reason for the increased expression of this circRNA. The regulation of tumor progression through the transcription factor activity of AR has been frequently reported in prostate cancer but is less documented in HCC (30-32). A study by Zhang *et al* (12) involving 142 patients with HCC found that 37% exhibited nuclear AR upregulation, which was clearly associated with poor patient prognosis, suggesting that

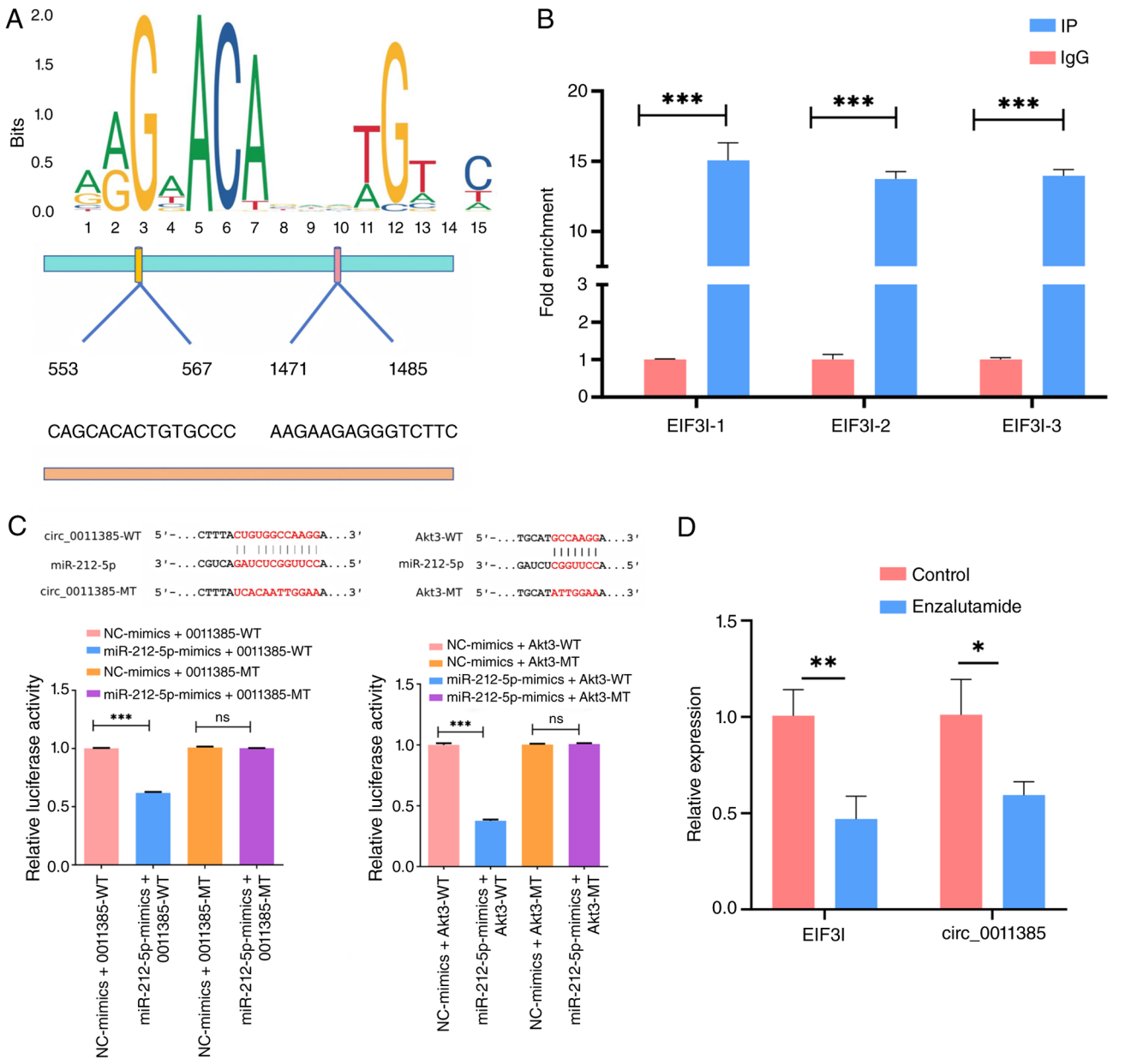

Figure 4. Mechanistic validation of the regulatory relationships within the AR/hsa_circ_0011385/miR-212-5p/Akt3 axis. (A) Schematic diagram of predicted androgen response elements in the promoter region of the EIF3I gene, generated using the JASPAR database. (B) Chromatin immunoprecipitation-qPCR assay determining the direct binding of AR to the EIF3I promoter at three predicted sites. IgG was used as a negative control. (C) Dual-luciferase reporter assays validating the direct interaction between miR-212-5p and hsa_circ_0011385 (left panel) or the 3'-UTR of Akt3 (right panel). WT and MT binding sites were used. (D) MHCC97H cells were treated with the AR antagonist enzalutamide (10 μM fpr 48 h) or DMSO control. Reverse transcription-quantitative PCR analysis showing that enzalutamide significantly reduced EIF3I mRNA (left) and hsa_circ_0011385 (right) expression levels. Data are presented as the mean ± SD from three independent experiments. *P<0.05, **P<0.01 and ***P<0.001. AR, androgen receptor; EIF3I, eukaryotic translation initiation factor 3 subunit I; miR, microRNA; MT, mutant; WT, wild-type; NC, negative control; IP, immunoprecipitation.

the transcription factor activity of AR may be an important factor in HCC progression. Recent research has also indicated that lenvatinib efficacy is suboptimal in patients with high AR levels but are AFP-negative, while combination therapy with the AR antagonist bicalutamide and lenvatinib can notably improve resistance (11). These conclusions support the present findings that the transcription factor activity of AR is closely associated with lenvatinib resistance.

Downstream, dual-luciferase reporter assays determined the direct targeting associations between hsa_circ_0011385 and miR-212-5p and between miR-212-5p and the Akt3 3'-UTR, forming a ceRNA regulatory network extending from transcriptional to post-transcriptional regulation. Functional experiments with the miR-212-5p mimic and inhibitor further demonstrated that miR-212-5p suppressed Akt3 expression, inhibited proliferation and promoted apoptosis in resistant cells, consistent with its role in the ceRNA axis. The present study indicated that Akt3 was the key downstream effector molecule in this AR-driven pathway. Extensive prior research has established the important role of Akt3, a key component of the PI3K/Akt signaling pathway, in HCC progression. Its activation has been shown to drive lenvatinib resistance by regulating a number of downstream substrates such as mTOR and GSK-3β (19-21,33-35). The

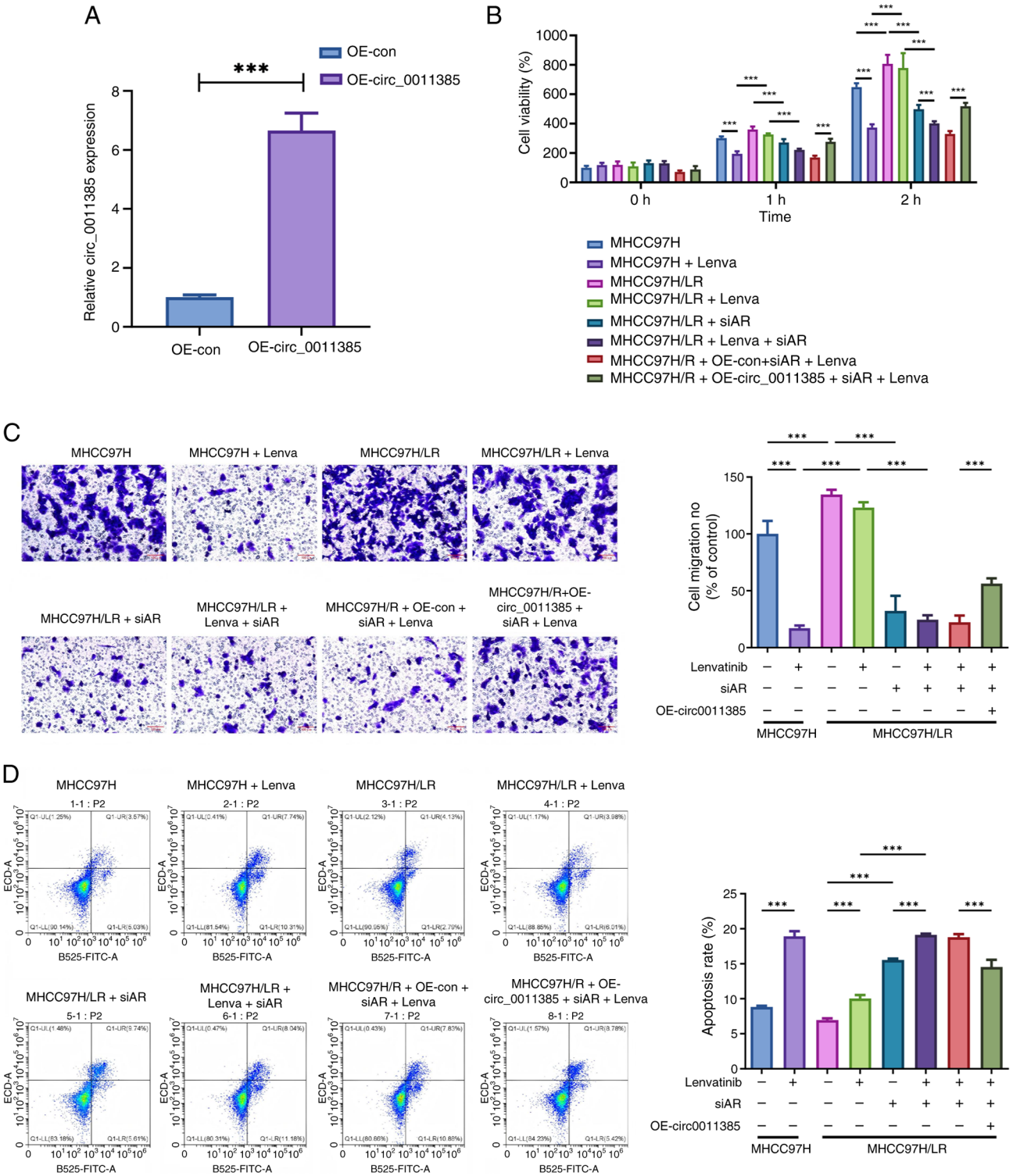

Figure 5. Functional role of AR and hsa_circ_0011385 in lenvatinib resistance. (A) Reverse transcription-quantitative PCR validation of hsa_circ_0011385 overexpression efficiency. Functional assays were performed in the following groups: MHCC97H parental cells with or without lenvatinib; MHCC97H-LR cells with or without lenvatinib; MHCC97H-LR cells transfected with si-AR, with or without lenvatinib; and MHCC97H-LR cells co-transfected with si-AR and oe-circ (or empty vector) plus lenvatinib. (B) Cell proliferation assessed by Cell Counting Kit-8 assay after lenvatinib treatment. (C) Cell mobility evaluated with Transwell chambers; representative fields (left) and pooled counts (right) are shown (scale bar, 100 μm). (D) Flow-cytometric apoptosis profiles (left, scatter plots; right, summary data). All values are presented as the mean ± SD from three independent experiments. ***P<0.001. AR, androgen receptor; si, small interfering; ns, not significant; oe, overexpression; con, control; circ; circular RNA; Lenva, lenvatinib; LR, lenvatinib-resistant.

present study did not aim to redundantly validate the detailed pathways downstream of Akt3 but focused on revealing a novel axis upstream of Akt3, where AR regulates circRNA through its host gene EIF3I.

Functionally, the present study found that AR knockdown significantly reversed the malignant phenotypes of resistant cells, including inhibiting proliferation and migration and promoting apoptosis. This beneficial effect was successfully

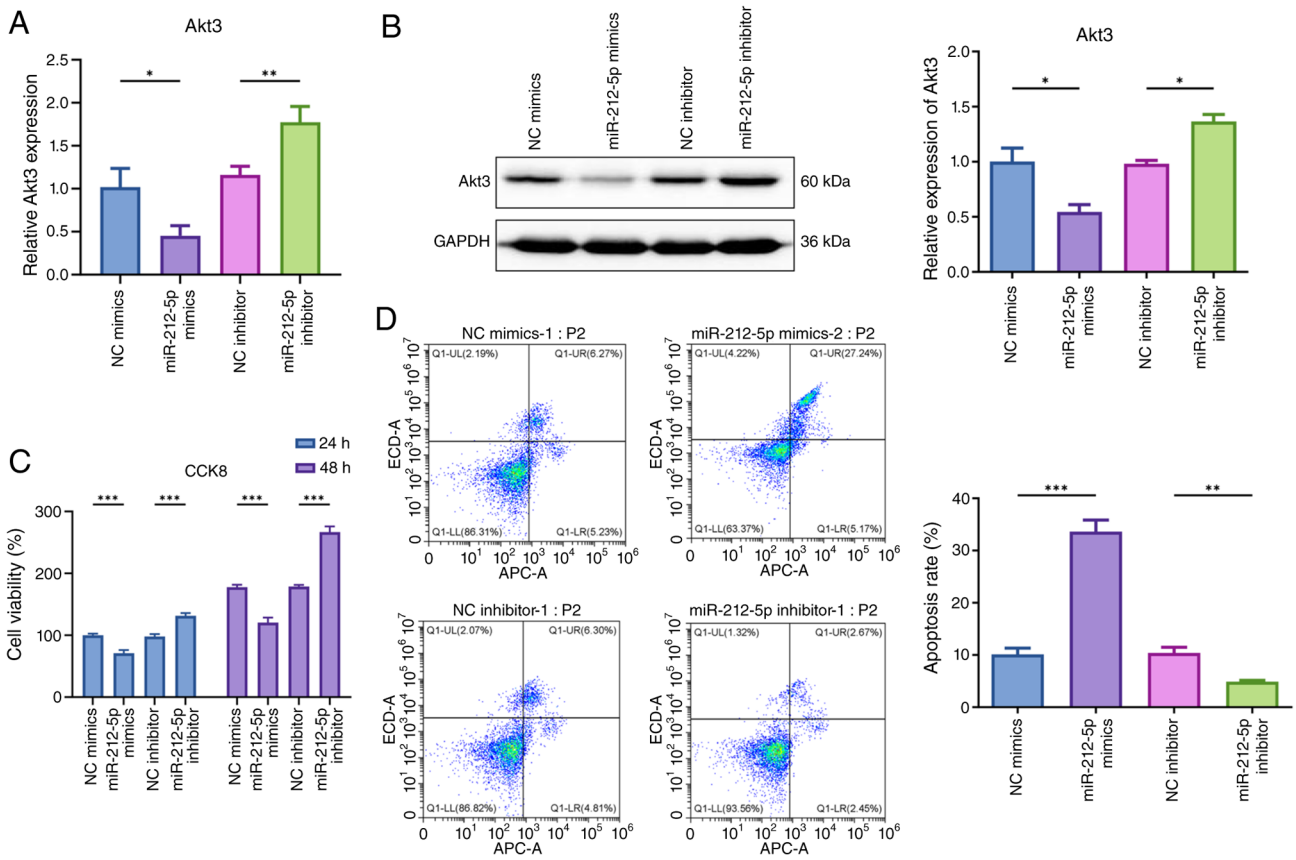

Figure 6. MiR-212-5p directly regulates Akt3 expression and lenvatinib sensitivity in MHCC97H-LR cells. (A) Reverse transcription-quantitative PCR analysis of Akt3 mRNA expression in MHCC97H-LR cells transfected with miR-212-5p mimic or inhibitor. (B) Western blotting analysis of Akt3 protein expression in MHCC97H-LR cells transfected with miR-212-5p mimic or inhibitor. GAPDH served as a loading control. (C) Cell proliferation assessed by a CCK-8 assay in MHCC97H-LR cells transfected with a miR-212-5p mimic or inhibitor, followed by treatment with increasing concentrations of lenvatinib for 72 h. (D) Flow cytometric apoptosis analysis of MHCC97H-LR cells transfected with miR-212-5p mimic or inhibitor after lenvatinib treatment. All values are presented as the mean ± SD from three independent experiments. *P<0.05, **P<0.01 and ***P<0.001 vs. respective NC group. miR, microRNA; NC, negative control; CCK-8, Cell Counting Kit-8; LR, lenvatinib-resistant.

reversed by exogenous overexpression of hsa_circ_0011385. This suggested that hsa_circ_0011385, driven by AR and produced through EIF3I transcription, is a key downstream effector in mediating lenvatinib resistance and suggests that targeting this specific node may have therapeutic potential.

The present study exhibited a number of limitations, the most notable being that the conclusions have not yet been validated in animal models or larger clinical cohorts. Furthermore, the mechanisms of lenvatinib resistance are highly heterogeneous and the AR/circ_0011385 axis may represent only one component. It is particularly important to note that the mechanism established in the present study was based on AR-high cell models; therefore, the present conclusions may primarily apply to the subset of patients with HCC and high AR expression. Whether this axis functions in AR-low or AR-negative HCC remains unclear and its interaction with other known resistance pathways warrants further exploration. Prospective clinical studies in lenvatinib-treated patients with HCC are needed to evaluate whether baseline expression levels of AR, hsa_circ_0011385 or Akt3 associate with treatment response and survival outcomes.

Despite these limitations, the present findings have important potential clinical implications. First, they suggest that AR expression levels and its regulated circRNA could serve as potential predictive biomarkers for lenvatinib efficacy in AR-high patients with HCC. Second, interventions targeting this pathway, such as using AR antagonists or specific oligonucleotides targeting hsa_circ_0011385, may represent novel strategies to overcome lenvatinib resistance in this specific patient subset in the future.

In summary, to the best of our knowledge, the present study revealed for the first time that in AR-high HCC, the AR drives the expression of its circRNA product hsa_circ_0011385 by directly transcriptionally activating its host gene, EIF3I. The highly expressed hsa_circ_0011385 functions by sequestering miR-212-5p, thereby alleviating its inhibitory effect on the downstream target gene Akt3, which ultimately activates pro-survival signaling pathways and confers lenvatinib resistance. These findings not only elucidate a complete AR-dominated ceRNA axis, spanning from transcriptional to post-transcriptional regulation, but importantly, establish a robust conceptual framework and highlight promising therapeutic targets. The present study therefore aids in identifying the subset of AR-high patients with HCC, predicting their lenvatinib response and devising combined treatment strategies (such as AR antagonists or circRNA-targeting therapies) against this pathway.

Acknowledgements

Not applicable.

Funding

The present study was supported by grants from the Medical Science and Technology Project of Zhejiang Province (grant no. 2022KY699) and the Chinese Medicine Research Program of Zhejiang Province (grant no. GZY-ZJ-KJ-24060).

Availability of data and materials

The data generated in the present study may be requested from the corresponding author.

Authors' contributions

CL and BZ conceived and designed the present study. MW, ZW and ZC performed the experiments. CL and YJ conducted the statistical analyses. BZ critically reviewed and revised the manuscript. CL, BZ and ZW prepared the figures. CL and BZ confirm the authenticity of all the raw data. All authors have read and approved the final version of the manuscript.

Ethics approval and consent to participate

Not applicable.

Patient consent for publication

Not applicable.

Competing interests

The authors declare that they have no competing interests.

References

1. Bray F, Laversanne M, Sung H, Ferlay J, Siegel RL, Soerjomataram I and Jemal A: Global cancer statistics 2022: GLOBOCAN estimates of incidence and mortality worldwide for 36 cancers in 185 countries. CA Cancer J Clin 74: 229-263, 2024.
2. Rumgay H, Arnold M, Ferlay J, Lesi O, Cabasag CJ, Vignat J, Laversanne M, McGlynn KA and Soerjomataram I: Global burden of primary liver cancer in 2020 and predictions to 2040. J Hepatol 77: 1598-1606, 2022.
3. Park JW, Chen M, Colombo M, Roberts LR, Schwartz M, Chen PJ, Kudo M, Johnson P, Wagner S, Orsini LS and Sherman M: Global patterns of hepatocellular carcinoma management from diagnosis to death: The BRIDGE study. Liver Int 35: 2155-2166, 2015.
4. Chen R, Hu X, Huang Y, Jiang Y, Chen G, Shan Q, Xu X and Zheng S: Regulated cell death in lenvatinib resistance of hepatocellular carcinoma: From molecular mechanisms to therapeutic strategies. Int J Biol Sci 21: 2012-2026, 2025.
5. Ye G, Ye M and Jin X: Roles of clinical application of lenvatinib and its resistance mechanism in advanced hepatocellular carcinoma (Review). Am J Cancer Res 14: 4113-4171, 2024.
6. Qin Y, Han S, Yu Y, Qi D, Ran M, Yang M, Liu Y, Li Y, Lu L, Liu Y and Li Y: Lenvatinib in hepatocellular carcinoma: Resistance mechanisms and strategies for improved efficacy. Liver Int 44: 1808-1831, 2024.
7. Tang L, Ji Y, Ni C, Xu Z, Shen Y, Lu H, Zhang C and Yang S: EIF4A3-mediated biogenesis of CircFADS1 promotes the progression of hepatocellular carcinoma via Wnt/β-catenin pathway. Adv Sci (Weinh) 12: e2411869, 2025.
8. Tang Y, Yuan F, Cao M, Ren Y, Li Y, Yang G, Zhong Z, Liang H, Xiong Z, He Z, *et al*: CircRNA-mTOR promotes hepatocellular carcinoma progression and lenvatinib resistance through the PSIP1/c-Myc Axis. Adv Sci (Weinh) 12: e2410591, 2025.
9. Yuan F, Tang Y, Liang H, Cao M, Ren Y, Li Y, Yang G, Zhong Z, Xiong Z, He Z, *et al*: CircPIK3C3 inhibits hepatocellular carcinoma progression and lenvatinib resistance by suppressing the Wnt/β-catenin pathway via the miR-452-5p/SOX15 axis. Genomics 117: 110999, 2025.
10. Dauki AM, Blachly JS, Kautto EA, Ezzat S, Abdel-Rahman MH and Coss CC: Transcriptionally active androgen receptor splice variants promote hepatocellular carcinoma progression. Cancer Res 80: 561-575, 2020.
11. Lin Z, Liu X, Wang H, Li S, Miao Z, Yang J, Zhang Y, Lei K, Wu Y, Kang Y, *et al*: Androgen receptor promotes arachidonic acid metabolism and angiogenic microenvironment in AFP-negative hepatocellular carcinoma. Nat Commun 16: 6451, 2025.
12. Zhang H, Li XX, Yang Y, Zhang Y, Wang HY and Zheng XFS: Significance and mechanism of androgen receptor overexpression and androgen receptor/mechanistic target of rapamycin cross-talk in hepatocellular carcinoma. Hepatology 67: 2271-2286, 2018.
13. Li X, Lv J, Hou L and Guo X: Circ_0001955 acts as a miR-646 sponge to promote the proliferation, metastasis and angiogenesis of hepatocellular carcinoma. Dig Dis Sci 67: 2257-2268, 2022.
14. Bai K, Ma Y and Li J: Circular RNA circ_0001955 promotes hepatocellular carcinoma tumorigenesis by up-regulating alkaline ceramidase 3 expression through microRNA-655-3p. Bioengineered 13: 2099-2113, 2022.
15. Fu D, Ji Q, Wang C, Yu L and Yu R: Aloin decelerates the progression of hepatocellular carcinoma through circ_0011385/miR-149-5p/WT1 axis. Cell Cycle 20: 2476-2493, 2021.
16. Ni C, Yang S, Ji Y, Duan Y, Yang W, Yang X, Li M, Xie J, Zhang C, Lu Y and Lu H: Hsa_circ_0011385 knockdown represses cell proliferation in hepatocellular carcinoma. Cell Death Discov 7: 270, 2021.
17. Hou W, Bridgeman B, Malnassy G, Ding X, Cotler SJ, Dhanarajan A and Qiu W: Integrin subunit beta 8 contributes to lenvatinib resistance in HCC. Hepatol Commun 6: 1786-1802, 2022.
18. Tian LY, Smit DJ and Jücker M: The role of PI3K/AKT/mTOR signaling in hepatocellular carcinoma metabolism. Int J Mol Sci 24: 2652, 2023.
19. Wang Z, Dou X, Shan Q, Ning Y, Wang J, Wang T, Cheng T, Shi K, Li S, Han X and Cao G: Targeting AKT to treat liver disease: Opportunities and challenges. Biochem Pharmacol 242: 117208, 2025.
20. Shu G, Su H, Wang Z, Lai S, Wang Y, Liu X, Dai L, Bi Y, Chen W, Huang W, *et al*: LINC00680 enhances hepatocellular carcinoma stemness behavior and chemoresistance by sponging miR-568 to upregulate AKT3. J Exp Clin Cancer Res 40: 45, 2021.
21. Jiang F, Lin Y, Du J, Qiu S, Luo G and Zhang Z: The transcription factor TBP promotes hepatocellular carcinoma progression by activating AKT3. Am J Cancer Res 13: 5656-5666, 2023.
22. Han D, Li J, Wang H, Su X, Hou J, Gu Y, Qian C, Lin Y, Liu X, Huang M, *et al*: Circular RNA circMTO1 acts as the sponge of microRNA-9 to suppress hepatocellular carcinoma progression. Hepatology 66: 1151-1164, 2017.
23. Liu Y, Dong Z, Chen W, Chen L, Ju L, Cai W, Luo X and Bian Z: Construction of a ceRNA regulatory network to explore potential pathogenesis mechanisms involved in human hepatocellular carcinoma. Sci Rep 13: 22058, 2023.
24. Ritchie ME, Phipson B, Wu D, Hu Y, Law CW, Shi W and Smyth G: limma powers differential expression analyses for RNA-sequencing and microarray studies. Nucleic Acids Res 43: e47, 2015.
25. Livak KJ and Schmittgen TD: Analysis of relative gene expression data using real-time quantitative PCR and the 2(-Delta Delta C(T)) method. Methods 25: 402-408, 2001.
26. Zhao J, Fang L, Pu R, Liu W, Cai S, Wang R, Shi Y, Li Z, Zhang Z, Li Z and Cao G: Androgen receptor-induced molecules and androgen contribute synergistically to male-predominance of hepatocellular carcinoma. iScience 27: 110519, 2024.

27. Yavuz M, Takanlou LS, Avcı ÇB and Demircan T: A selective androgen receptor modulator, S4, displays robust anti-cancer activity on hepatocellular cancer cells by negatively regulating PI3K/AKT/mTOR signalling pathway. Gene 869: 147390, 2023.
28. Wei X, Si A, Zhao S, Fu Y, Li J, Aishanjiang K, Ma Y, Yu C, Yu B, Cui C, *et al*: CircUCK2(2,3) promotes cancer progression and enhances synergistic cytotoxicity of lenvatinib with EGFR inhibitors via activating CNIH4-TGFα-EGFR signaling. Cell Mol Biol Lett 30: 15, 2025.
29. Abudoureyimu M, Sun N, Chen W, Lin X, Pan F and Wang R: Aurora-A promotes lenvatinib resistance experimentally through hsa-circ-0058046/miR-424-5p/FGFR1 axis in hepatocellular carcinoma. Int J Immunopathol Pharmacol 39: 3946320251316692, 2025.
30. Wang Q, Wu Y, Long Y, Li R, Shi Y, Zheng Y, Chen X, Li X, Zhou Y, Huang X and Jiang G: AR+TREM2+ macrophage induced pathogenic immunosuppression promotes prostate cancer progression. Nat Commun 16: 6964, 2025.
31. Xu P, Yang JC, Chen B, Nip C, Van Dyke JE, Zhang X, Chen HW, Evans CP, Murphy WJ and Liu C: Androgen receptor blockade resistance with enzalutamide in prostate cancer results in immunosuppressive alterations in the tumor immune microenvironment. J Immunother Cancer 11: e006581, 2023.
32. Chukhu M, Dahiya UR and Heemers HV: Evolving roles for the androgen receptor and its protein interactome in castration-resistant prostate cancer. Oncogene 44: 3883-3894, 2025.
33. Tang Y, Fan S, Peng R, Liu H, Su B, Tu D, Wang S, Jin X, Jiang G, Jin S, *et al*: TRIM29 reverses lenvatinib resistance in liver cancer cells by ubiquitinating and degrading YBX1 to inhibit the PI3K/AKT pathway. Transl Oncol 53: 102294, 2025.
34. Wang J, Shi J, Mi L, Zhao M, Han G and Yin F: Aberrant activation of the PI3K/AKT/HIF-1α pathway promotes glycolysis and lenvatinib resistance in liver cancer. Mol Med Rep 32: 301, 2025.
35. Tian LY, Smit DJ, Popova NV, Horn S, Velasquez LN, Huber S and Jücker M: All three AKT isoforms can upregulate oxygen metabolism and lactate production in human hepatocellular carcinoma cell lines. Int J Mol Sci 25: 2168, 2024.